Anisotropic Mechanical Behavior of Magnetically Oriented Iron Particle Reinforced Foams

L. Sorrentino, M. Aurilia, G. Forte, S. Iannace

Institute for Composite and Biomedical Materials (IMCB), National Research Council, Piazzale Enrico Fermi 1, 80055 Portici (NA), Italy

Received 3 February 2010; accepted 12 April 2010
DOI 10.1002/app.32603
Published online 18 August 2010 in Wiley Online Library (wileyonlinelibrary.com).

ABSTRACT: Reinforced foams were prepared by exposing a polyurethane matrix filled with iron particles to a magnetic field during the foaming process. The magnetic field induced an alignment of the iron particles along the field direction, giving rise to columnar structures similar to fibrils, as observed by SEM and microtomographic 3D reconstructions. The anisotropic reinforcement induced by the fibrils improved the mechanical performances, yielding a threefold increase of both elastic modulus and yield stress in the alignment direction, whereas minor effects were observed in the transversal direction. In this case, the mechanical properties were comparable with those of randomly filled foams or, in some cases, of unfilled foam. The reinforcing efficiency of fibrils was evaluated through a theoretical model, based on the combination of the mechanics of foams with two micromechanical models for aligned short fibers composites (Halpin-Tsai and Cox-Krenchel). The theoretical predictions based on the Halpin-Tsai equations showed a good agreement with the experimental data, whereas the model derived from Cox-Krenchel equations overestimated data. © 2010 Wiley Periodicals, Inc. J Appl Polym Sci 119: 1239–1247, 2011

Key words: foams; mechanical properties; composites; magnetic polymers; reinforcement

INTRODUCTION

Polymeric foams are employed in several nonstructural (such as packaging, shock absorbing, cushioning, thermal, and acoustic insulation)[1,2] and structural applications (such as sandwiches), where lightweight and high-stiffness to weight ratio are required.[3] Elastic modulus, yield point,[3] and length of stress plateau[4,5] are the main parameters to be considered in foam design for specific applications.

Mechanical properties of foams are strongly related to the expansion ratio (defined as the ratio between foam density and bulk polymer density) and to the cell morphology.[6] The regularity of cell shape is mostly influenced by the foaming process, in particular when foams expand in a mold, and the geometrical constraints hinder the cells to grow with spherical shape.

The mechanical behavior of the foams with anisotropic cells changes according to the load direction, being higher in the direction of elongated cells.[7] In this case, in fact, the axial response of struts and walls of cells is maximized. The yield point and the plateau region are shifted toward higher stress values, because the edge buckling takes place under higher loads. As a general rule, to enhance the mechanical response in a preferential direction, the structure instabilities should be reduced, as widely evidenced and modeled in literature.[6,8,9] It is worth to outline that, even if some degree of anisotropy is induced by all conventional foaming processes, isotropic mechanical performances are usually exhibited by foams.

The conventional methods used to improve the mechanical response of foams fall within two main categories: (a) the increase of the matrix elastic properties, by incorporating a filler, such as particles or fibers, in the polymeric matrix and (b) the insertion of structural reinforcements after the foaming process. In the former approach, isotropic materials with moderate increase of structural properties are obtained when low-filler content is added[10–12] or low-foam density is reached.[13] When high-filler content is used to strongly rise the mechanical response,[14,15] difficulties are experienced, because of the poor control of the cellular morphology and the filler interference during the morphology development, and low-expansion ratios are obtained, because of the hindering effect of the reinforcement on the bubble growth process. Furthermore, when high mechanical responses of cellular structures are required in a preferential direction, the isotropic dispersion is not the most efficient way to exploit the filler reinforcement. Mechanical property measurements in carefully fabricated aligned and random composites have shown that aligned fibers were 90% more effective at stiffening the composite (in the

Correspondence to: L. Sorrentino (luigi.sorrentino@cnr.it).

alignment direction) than were randomly oriented fibers.[16]

When the approach based on the insertion of rigid reinforcements is employed, metallic pins[17–21] and stitch bonds[22,23] are the most used methods to reinforce composite structure, such as in some sandwich applications. These methods are mechanically effective but needs a complex and long postprocessing step, which rises costs[16] and can damage the integrity of foam layer during pin insertion (e.g. 0.5 mm thick pins are used in).[18] Moreover, this technique leads to an increase of the overall core density because of pins weight.

A very effective method to control the mechanical behavior of a polymeric matrix is the use of reinforcing fillers, capable of being oriented by the magnetic field, as occurs in magnetorheological fluids[24] and magnetoelastomers.[25,26] The formation of columnar structures (fibrils), through the application of a magnetic field, can change the rheological behavior of the fluid and even completely block the flow. This technique was successfully adopted to control the mechanical behavior of silicone based magnetoelastomers.[13,24–27] The anisotropy of the mechanical properties was induced during the consolidation of the silicon matrix by aligning, under the application of a magnetic field, the iron particles along a preferential direction. The elastic moduli of these composite materials strongly increased in the alignment direction.[24–26]

Recently, some works were done on magnetorheological gels, which were characterized by a low-elastic modulus, with the scope of producing springless dampers.[28]

In this work, we present a new, cost effective method to prepare reinforced foamed structures characterized by an high mechanical anisotropy. The mechanical response of the porous structure can be easily tailored by means of a one step process, according to the proper orientation of the particles without interfering with the formation of the cellular morphology. The concept was demonstrated by preparing and characterizing foams based on a flexible polyurethane by exploiting the reinforcing effect of low amount of aligned iron particles.

This approach could be used in all applications of porous or foamed structures, where a tailored mechanical anisotropy is required. In fact, a good adhesion is retained between the polymeric matrix and the reinforcing phase after the foaming process, without the introduction of cracks or, at least, without affecting the regularity of the cellular morphology. Among the potential fields, this concept could be employed in the biomedical field, to prepare engineering scaffold in bone tissues,[29,30] or in sandwich structures applications, in which the proper orientation of the filler could drastically increase both elastic and ultimate shear properties of the core.[18,21]

TABLE I
Physical Properties of Foam Components

Material	PU	Iron particles
Density [kg dm^{-3}]	1.05	7.80
Elastic Modulus [GPa]	0.10	211
Mean diameter [μm]		20

EXPERIMENTAL

Open cell PU-foams were prepared by using polyalcohol (Bayfit 14,902/AO) and diisocyanate (Desmodur M-54) components, both supplied by BaySistems Italia (Italy). Iron microparticles (particle size lower than 44 μm) were purchased from Sigma Aldrich (Milano, Italy). The physical properties of the used materials are summarized in the Table I.

Iron particles were mixed with the polyalcohol in a flask for 5 min at 2000 RPM to obtain an homogeneous particle dispersion. Diisocyanate was then added to the Fe/Polyalcohol mixture and intimately mixed before being injected in a 50 × 50 × 30 mm^3 PTFE mold.[31]

Five weight percentages (from 5 to 25) of iron particles were used to investigate the effect of particle content. Three series of foam samples were prepared: (a) without the MF application (Randomly Dispersed particles samples-RD), (b) with the MF application along the vertical direction (Fig. 1), parallel to the foam growth direction (samples with particles Aligned in Vertical direction-AV), and (c) with the MF application along the horizontal direction (Fig. 1), transversal to the foaming growth direction (samples with particles Aligned in Horizontal direction-AH).

The MF was generated by two permanent magnets (coercivity = 10,500 Oe, remanence = 11,700 G) purchased from Magneti Permanenti Italia, Italy. The MF was applied by positioning magnets at opposite faces of the mold (according to the reference directions shown in Fig. 1) during the foaming process. The experimental plan is reported in Table II.

The mechanical compressive behavior was analyzed through a dynamometer (CMT-4304 from SANS, China) equipped with a 1 kN load cell and setting the crosshead speed to 50 mm min^{-1}. All foam samples were tested both in vertical and horizontal directions, to evaluate the mechanical behavior either in the alignment direction or in the orthogonal one and to estimate the mechanical anisotropy of the foams. Compression tests were performed on 20 mm edge cubic samples, cut from the core of foam samples to reduce the influence of the boundary effects related to the morphological

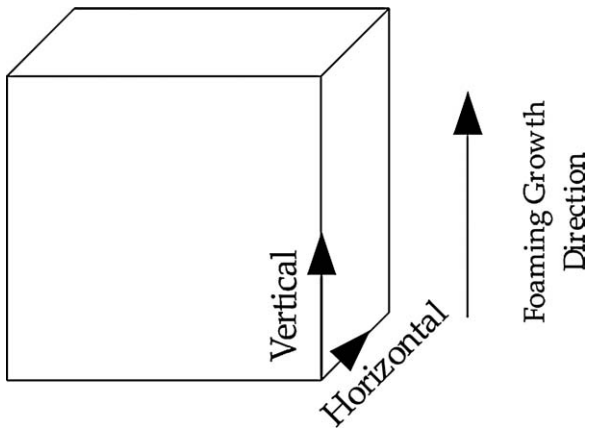

Figure 1 Reference directions. The magnetic field was applied in the horizontal or vertical directions.

inhomogeneity of the sample walls. Three samples for each configuration were tested, and the average values and standard deviations were evaluated.

Foams morphologies were analyzed by using both optical (PlanApo MZ16, from Leica MicroSystems, Germany) and scanning electron (S440, from Leica MicroSystems, Germany) microscopes. 3D microtomography acquisitions and reconstructions were carried out to evaluate the 3D morphology of some samples. Tomographic images were acquired through the Syrmep BeamLine at the Sincrotrone Trieste Facility (Trieste, Italy), and 3D volumes were reconstructed with a commercial software available at the Syrmep BeamLine.

Finally, the statistical analysis of the length distribution of columnar structures was performed on images obtained from optical analysis.

TABLE II
Compositions of Foams and Directions of the Magnetic Field Application

		Iron content [%]		
	Sample	by weight	by volume	MF direction
Neat PU		0	0	No
RD series	Fe5	5	0.64	No
	Fe10	10	1.28	No
	Fe15	15	1.92	No
	Fe20	20	2.56	No
	Fe25	25	3.21	No
AV series	Fe5	5	0.64	Vertical
	Fe10	10	1.28	Vertical
	Fe15	15	1.92	Vertical
	Fe20	20	2.56	Vertical
	Fe25	25	3.21	Vertical
AH series	Fe5	5	0.64	Horizontal
	Fe10	10	1.28	Horizontal
	Fe15	15	1.92	Horizontal
	Fe20	20	2.56	Horizontal
	Fe25	25	3.21	Horizontal

RESULTS AND DISCUSSION

Morphological analysis

The foam samples were produced by keeping constant the mass of the mixture injected in the mold. The different amount of iron particles influenced significantly the final morphology of the cellular structures as evidenced by the comparison with the cellular morphologies of three foam samples (iron content 15, 20, and 25% by weight, Fig. 2). Indeed, as the weight percentage of iron particles raised, a lower amount of polymer was available to build up the cellular structure. As an example, in the samples containing 25% by weight of iron particles the polymer amount was 75% of that of the unfilled PU

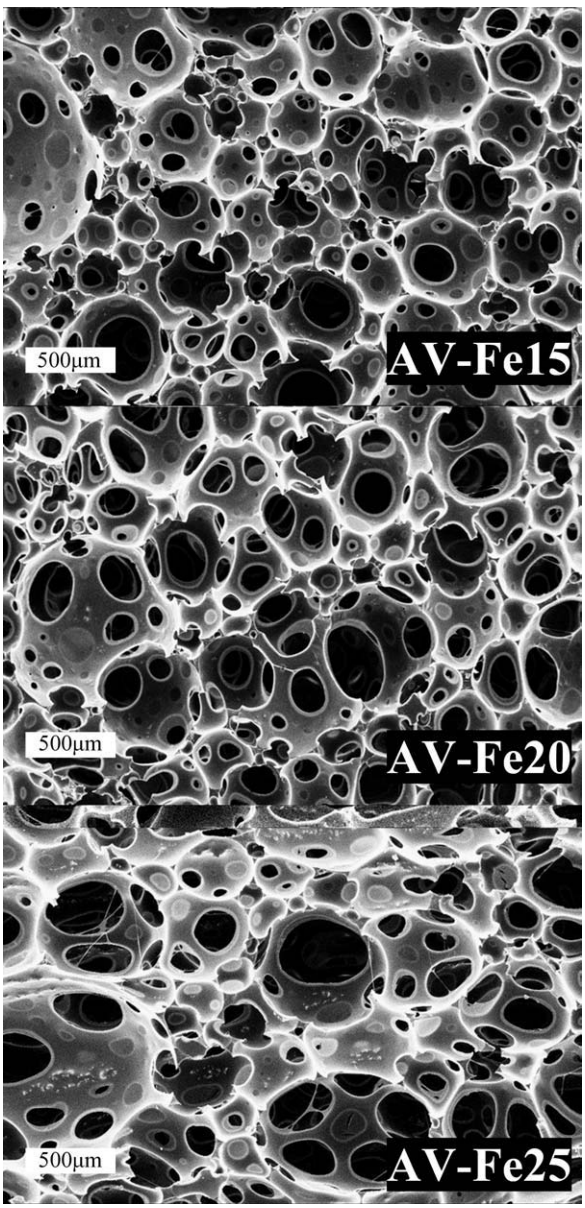

Figure 2 SEM micrographies of particle filled foams (samples AV-Fe15, AV-Fe20, AV-Fe25).

TABLE III
Foam Densities of AV-Foams

Iron particles weight content [%]	Iron particles volume content [%]	Foam density [g cm^{-3}]
0		0.10
5	0.63	0.13
10	1.25	0.14
15	1.87	0.13
20	2.48	0.10
25	3.08	0.06

sample. As a result, both mean cell diameter and porosity increased (Fig. 2); whereas, the actual foam density was reduced, as reported in Table III.

To show how the iron particles were aligned along the flux lines of the MF, microcomputed tomography analysis was performed on selected samples. The observation of the reconstructed 3D volumes from the acquired data evidenced the aligning effect of the MF during the foaming process, which resulted in the fibrillar rearrangement of the filler [Fig. 3(C)]. On the contrary, the samples produced without the MF exhibited a random distribution of the filler [Fig. 3(B)] in the polymeric matrix [Fig. 3(A)].

The SEM analysis of the cellular struts showed that iron particles protruded from the struts surfaces both in the sample with randomly distributed [RD sample, Fig. 4(A)] and in that with aligned [AV sample, Fig. 4(B)] particles. The iron particles were homogeneously distributed within the struts (included the transversal ones) in RD-foams; whereas, in AV-foams, iron particles were prevalently present in vertical struts inducing an high structural anisotropy, whose effects will be evidenced by the mechanical characterization.

It is interesting to note that, the lengths of the fibrillar structures were directly related to the particle content, as evident from the comparison with the different samples in Figure 5, and that fibrils were longer than the mean cells diameters, resulting in an effective structural reinforcement through adjacent cells, as discussed in the following.

Mechanical characterization

The addition of iron particles reinforced the foams structure, and, as expected, both elastic modulus and yield stress increased (Table IV). The samples filled with randomly dispersed particles showed an increase of the overall mechanical response with the particle contents, when compared with the neat PU. The RD-Fe15 sample (15%wt of iron particles) presented the highest elastic modulus and yield stress of the RD series. At higher particle contents, a decrease of the mechanical parameters was detected, although the amount of iron particles and the fibrils length increased (Fig. 5). This behavior was related to the growth of the expansion ratio induced by the reduction of the polymeric phase, which caused a more porous structure as previously evidenced. As clearly stated by the mechanics of open cell foams, both elastic modulus and yield stress depend on the square of the expansion ratio (see Eq. (1) in the analysis section), so the effect of density reduction on the mechanical response was predominant over the matrix reinforcement induced by the increased iron content.

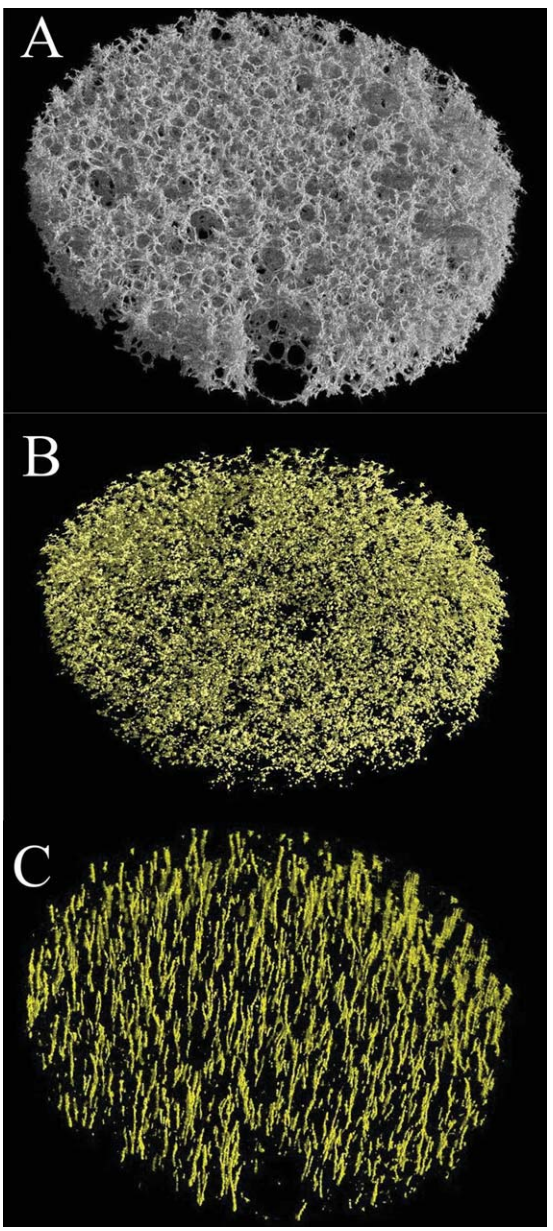

Figure 3 3D volume reconstruction of: neat PU-foam (A), randomly dispersed iron particles in RD-foam (B), and aligned iron particles (fibrils) in AV-foam (C) [Color figure can be viewed in the online issue, which is available at wileyonlinelibrary.com.]

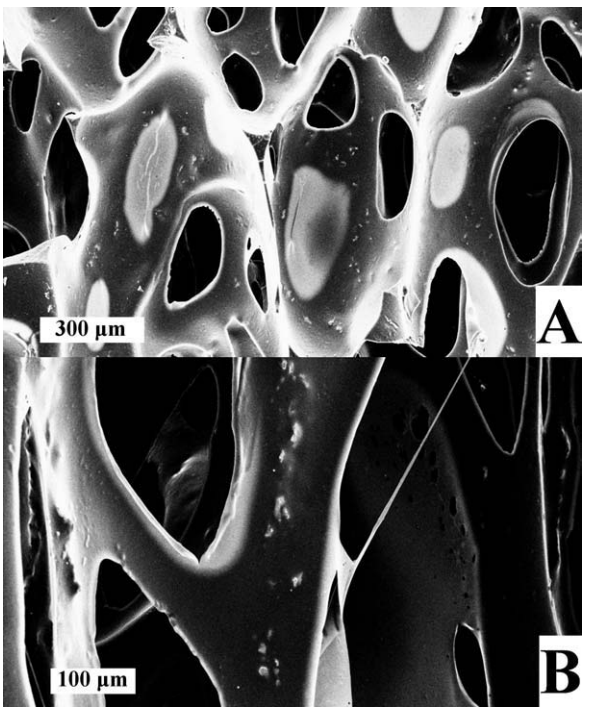

Figure 4 SEM micrographies of RD and AV samples showing the iron particles protruding from the struts.

In samples prepared by applying the MF, the mechanical behavior was strongly influenced by the direction of the fibrillar structures developed. The AV-Fe15 sample exhibited a threefold increase of the elastic modulus when compared with the elastic modulus of the neat PU (Fig. 6). On the contrary, the compressive tests performed along the orthogonal direction to the MF lines showed that the filler slightly reinforced the matrix and the resulting stress-strain curve was comparable to that of the RD samples (Fig. 7). This was ascribed to the low amount of iron particles in all the struts orthogonal to the MF direction.

TABLE IV
Mechanical Properties (Elastic Modulus, *E*; Yield Stress, σ_{yield}) of Foam Samples

	Vertical		Horizontal	
Directions	*E* [kPa]	σ_{yield} [kPa]	*E* [kPa]	σ_{yield} [kPa]
Neat PU	110 ± 5.5	9.7 ± 1.0	115 ± 10.4	10.1 ± 0.8
RD-Fe5	97 ± 7.8	10.6 ± 0.7	102 ± 8.2	11.3 ± 1.0
RD-Fe10	122 ± 8.5	13.9 ± 1.1	124 ± 9.9	13.3 ± 1.1
RD-Fe15	253 ± 25.3	20 ± 1.0	248 ± 22.3	18 ± 1.8
RD-Fe20	116 ± 5.8	12.8 ± 0.8	123 ± 11.1	12.9 ± 1.0
RD-Fe25	79 ± 4.0	8.2 ± 0.7	81 ± 4.1	8.8 ± 0.5
AV-Fe5	189 ± 11.3	15.3 ± 1.2	121 ± 8.5	12.8 ± 1.0
AV-Fe10	222 ± 13.3	17.8 ± 1.4	145 ± 8.7	14.7 ± 1.0
AV-Fe15	313 ± 25.0	23.9 ± 2.2	170 ± 15.3	16.1 ± 1.1
AV-Fe20	278 ± 13.9	25 ± 1.5	116 ± 10.4	10.8 ± 1.0
AV-Fe25	135 ± 13.5	15.4 ± 0.8	40 ± 2.8	5.3 ± 0.4
AH-Fe5	98 ± 8.8	9.9 ± 0.6	94 ± 4.7	9.9 ± 0.7
AH-Fe10	110 ± 9.9	11.8 ± 1.2	251 ± 20.1	23.6 ± 1.7
AH-Fe15	134 ± 13.4	14 ± 1.1	391 ± 23.5	33.1 ± 1.7
AH-Fe20	113 ± 6.8	9.9 ± 0.7	339 ± 20.3	29.2 ± 2.6
AH-Fe25	40 ± 3.2	5.6 ± 0.3	278 ± 22.2	22.5 ± 1.1

To show how a stronger MF affected the mechanical response of the reinforced foams, the AH-foam series was prepared by applying the MF in the orthogonal direction to foam growth and reducing the distance between permanent magnets. As reported in Table IV, the trends of elastic modulus and yield stress were the same of the AV series, also in this case showing a maximum at 15%wt of particle

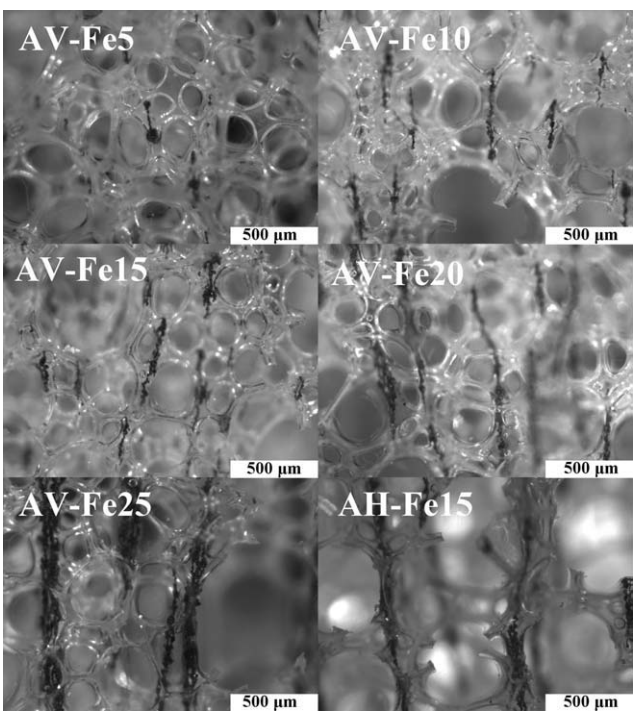

Figure 5 Optical micrographies of AV samples with different iron particles content and AH-Fe15 sample.

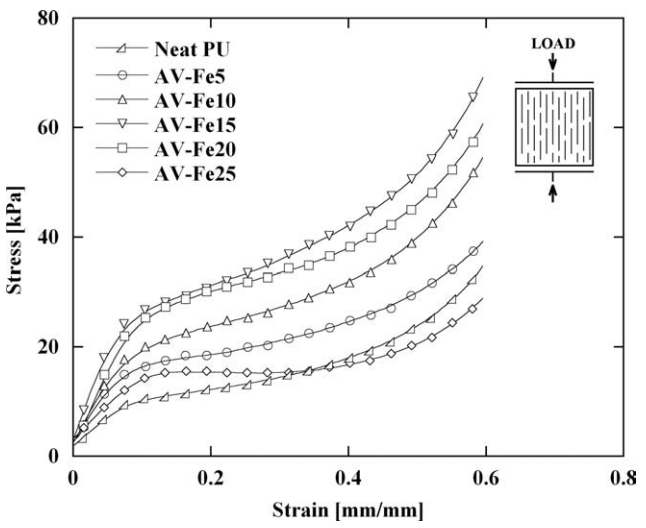

Figure 6 Stress-strain curves in MF direction of the AV-foam samples and of the unfilled foam.

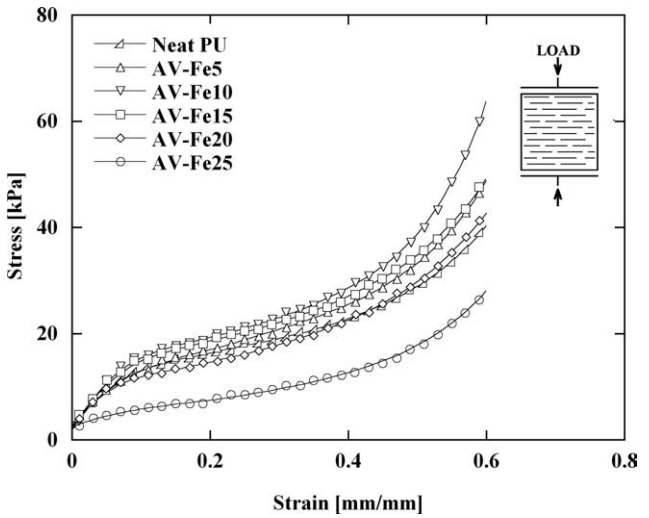

Figure 7 Stress-strain curves in orthogonal direction to MF of the AV-foams and of the unfilled foam.

content (both in parallel and orthogonal to MF directions), but the elastic modulus and the yield strength values were further shifted toward higher values. This was attributed to the increased intensity of MF in the horizontal direction with respect to that applied in the vertical one (as a consequence of the lower distance between permanent magnets), which resulted in longer fibrils in the horizontal direction as confirmed by optical images of fibrils of AV-Fe15 and AH-Fe15 samples (Fig. 5), and to an higher regularity of cell morphology detected by low-magnification optical images (not reported). In fact, when the MF and the foam growth directions were perpendicular, the mutual influence between fibrils formation and cell growth process was lower. As a consequence, a more effective reinforcement of the cellular structure in the alignment direction was obtained in AH samples and the weakening of the struts in the perpendicular direction was further increased with respect to AV samples.

In Figure 8, the stress-strain curves of all samples containing 15%wt of iron particles are compared with that of the neat PU. The addition of less than 2% by volume (corresponding to 15% by weight) of iron particles induced an increase of the mechanical response (RD-Fe15), but when the MF was applied during the foaming process a very high mechanical properties increase was obtained. In particular, the AH-Fe15 sample exhibited the highest elastic modulus and yield strength (more than threefold that of the neat PU-foam) in the particle alignment direction.

Analysis of mechanical behavior of AV-foams

The reinforcing efficiency induced by the fibrillar structures was evaluated by comparing the experimental measurements with the predictions of a theoretical model developed on the hypothesis of foams reinforced with iron microfibers having the same mean dimensions of the fibrils.

The elastic moduli of the particle filled matrices were evaluated by means of the Eq. (1) rearranged from Gibson and Ashby,[7] which relates the elastic modulus of the matrix to both elastic modulus and expansion ratio of the foam:

$$E_m = \frac{1}{k}\left(\frac{\rho_m}{\rho_f}\right)^2 E_f \quad (1)$$

where k is a constant close to 1, E, and ρ are the elastic modulus and the density of the matrix (m subscript) and the foam (f subscript), respectively. The value of the constant k used in this work was equal to 1. Equation (1) was inverted with respect to the usual expression, that shows the dependence of the foam elastic modulus from that of the matrix. The density of particle filled matrices was calculated through the rule of mixture from the physical properties of the components (from Tables I and II), whereas densities and elastic moduli of foams were measured (Table III).

The elastic moduli ratio (EMR) between the elastic modulus of the particle filled matrix (pm subscript) and the elastic modulus of the neat polymer matrix (m subscript) was related to the ratio between the elastic modulus of the particle filled foams (pf subscript) and the modulus of the neat PU-foams (f subscript), according to Eq. (2):

$$\mathrm{EMR} = \frac{E_{pm}}{E_m} = \left(\frac{\rho_{pm}}{\rho_{pf}}\frac{\rho_f}{\rho_m}\right)^2 \frac{E_{pf}}{E_f} \quad (2)$$

where ρ_{pf} and ρ_{pm} are the densities of the particle filled foam and its matrix, E_{pf} and E_{pm} are the elastic

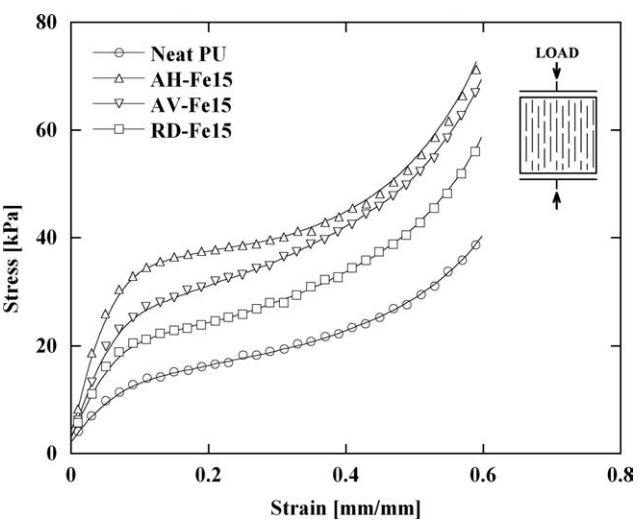

Figure 8 Stress-strain curves of 15% wt samples and of the neat PU-foam.

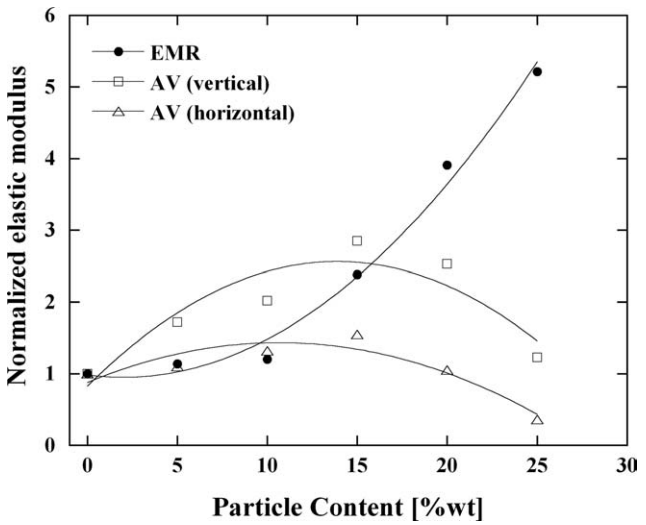

Figure 9 EMR (round marker) and normalized elastic moduli of AV samples in vertical (parallel to MF, square marker) and horizontal (orthogonal to MF, triangular marker) directions (Continuous lines are parabolic regressions).

moduli of the particle filled foam and of its matrix, respectively.

The EMR was calculated to evaluate the fibril reinforcement in the matrix. It showed a monotonic increase with the filler content (round marker in Fig. 9), in contrast with the normalized moduli of the same foams both in the vertical and horizontal directions (square and triangular markers, respectively, in Fig. 9) which presented a maximum at 15% filler content.

The elastic modulus of iron particles is very high with respect to that of the polymer, hence the hypothesis that the iron fibrils behaved as continuous short iron fibers for small deformations was assumed. The elastic modulus of the matrix increases as function of both aspect ratio and content of iron fibrils. Its behavior was described by means of two well-known micromechanical models for reinforced composites with aligned short fibers: Halpin-Tsai[32,33] and Cox-Krenchel[33–35] models. The first one is a self-consistent method described by the following equations:

$$\frac{E_{pm}}{E_m} = \mathrm{EMR} = \frac{1 + \zeta\eta\phi_i}{1 - \eta\phi_i} \tag{3}$$

$$\eta = \frac{\frac{E_i}{E_m} - 1}{\frac{E_i}{E_m} + \zeta} \tag{4}$$

where E_{pm}, E_i, and E_m are the elastic moduli of reinforced matrices, of the iron fibrils (considered as short fibers), and of the neat PU, respectively; ζ is the aspect ratio of iron fibrils and φ_i is their volume fraction. The Cox-Krenchel model, derived by the shear lag model,[33] evaluates the elastic modulus of the composite (E_{pf}) using a modified 'rule of mixtures' equation:

$$\frac{E_{pm}}{E_m} = \eta_0\eta_1\phi_i\frac{E_i}{E_m} + (1 - \phi_i) \tag{5}$$

where E_{pm}, E_i, and E_m are the elastic moduli of the reinforced matrices, of the iron fibrils (considered as short fibers) and of the neat PU, respectively. φ_i is the fibril volume fraction, η_0 is the Krenchel orientation factor ($\eta_0 = 1$ for reinforcement aligned in one direction) and η_1 is the Cox fiber length efficiency factor:

$$\eta_1 = \left[1 - \frac{\tanh\left(\beta\frac{L}{2}\right)}{\beta\frac{L}{2}}\right] \tag{6}$$

with

$$\beta = \frac{2}{D}\left(\frac{2G_m}{E_i \ln\sqrt{\frac{\pi}{4\Phi_i}}}\right)^{1/2} \tag{7}$$

where L is the fibrils length, G_m is the shear modulus of the matrix given by $G_m = E_m/2(1 + \upsilon)$, υ is the Poisson ratio of the polymeric matrix of the foam. The Poisson ratio used for the calculations was 0.45 assuming an elastomeric behavior of the polymeric matrix. However, the variation of the predicted values of Eq. (5) was smaller than 2% for Poisson ratio ranging between 0.33 and 0.5.

The Eq. (8), derived from the Halpin-Tsai model, and the Eq. (9), derived from the Cox-Krenchel model, were obtained by the combination of the Eqs. (3) and (5) with the Eq. (2), respectively:

$$\frac{E_{pf}}{E_f} = \left(\frac{\rho_{pf}}{\rho_{pm}}\frac{\rho_m}{\rho_f}\right)^2\frac{1 + \zeta\eta\phi_i}{1 - \eta\phi_i} \tag{8}$$

$$\frac{E_{pf}}{E_f} = \left(\frac{\rho_{pf}}{\rho_{pm}}\frac{\rho_m}{\rho_f}\right)^2\left[\eta_0\eta_1\phi_i\frac{E_i}{E_m} + (1 - \phi_i)\right] \tag{9}$$

They show the dependence of the mechanical behavior of the reinforced foams upon both aspect ratio and volume fraction of fibrils in the matrix and were used to evaluate the aspect ratio of fibrils within the foams.

The actual distributions of iron fibril lengths within the foams were measured by means of optical microscope analysis. For each foam the length of 30 fibrils were detected, and their mean length was determined as function of particles content. The mean value of each distribution was divided by the average iron particle diameter (Table I) and the aspect ratio distribution of iron fibrils was obtained (Fig. 10).

The comparison of the iron fibrils mean aspect ratio obtained from the optical analysis with those

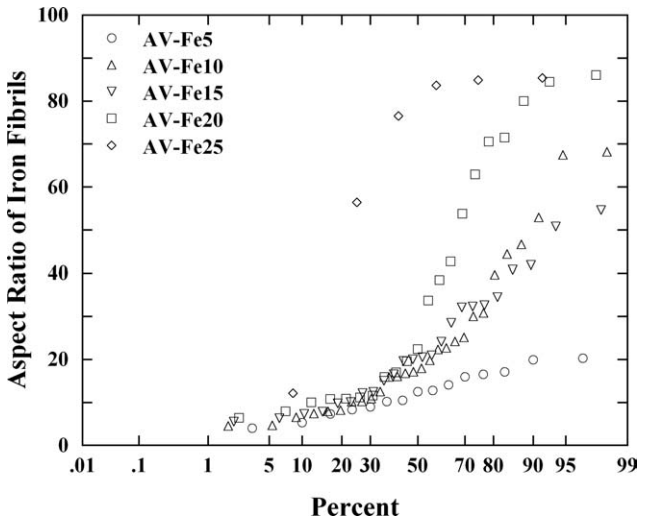

Figure 10 Aspect ratio distributions of iron fibrils within AV-foams.

evaluated by means of both Halpin-Tsai and Cox-Krenchel equations is shown in Figure 11. The results provided by the Halpin-Tsai model are in agreement with the experimental data at all particle contents and the predicted values are included within the standard deviation range at all concentrations. The theoretical predictions obtained from the Cox-Krenchel model are much higher than both experimental data and Halpin-Tsai model. The discrepancies between the two employed theoretical models have been also detected elsewhere,[33] where it was pointed out that Halpin-Tsai equations are more accurate for reinforced systems containing very short fibers, whereas the models derived by the shear lag model (such as the Cox-Krenchel model) is

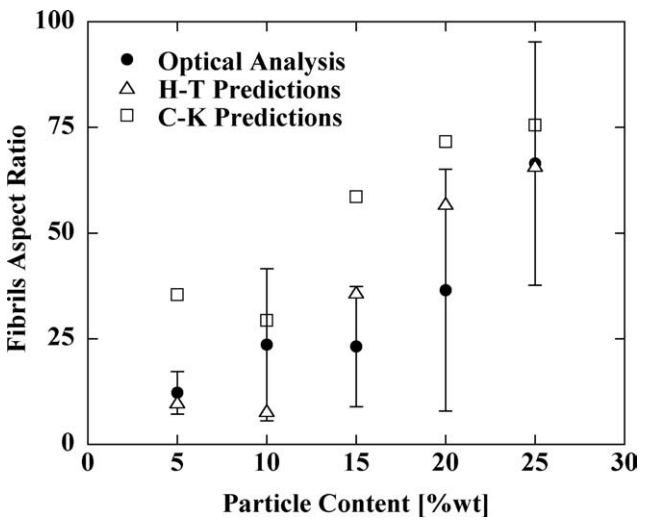

Figure 11 Aspect ratios of fibrils measured from optical micrographies and estimated by both Halpin-Tsai [Eq. (8)] and Cox-Krenchel [Eq. (9)] models.

reliable when the fibers are long (since the shear lag theory treats the fiber as a slender body).

However, both theoretical models predicted a mean aspect ratio of the iron fibrils comparable with or even higher than the experimental one, demonstrating that the reinforcing efficiency of the iron fibrils was as high as that of continuous short fibers with equivalent aspect ratios.

As a final consideration, the foaming process used in this work allowed to reach mechanical performances as high as those theoretically predicted for aligned short fibers reinforced foams, but with the advantage that the iron fibrils did not affected the foam integrity, being simultaneously formed with foam cells during the foaming process.

CONCLUSIONS

The mechanical behavior of open cell foams based on polyurethane matrix and reinforced with iron microparticles was analyzed. The effect of the MF application during the foaming process on the mechanical reinforcement was also investigated. Iron particles rearranged in fibrillar structures aligned along the field lines when the MF was applied, as evidenced by SEM analysis and 3D microCT volume reconstructions.

The foams prepared with a random dispersion of microparticles showed mechanical performances higher than the unfilled PU-foam, but when the fibrils where developed by applying a MF during the foaming process, strong improvements of the stress-strain behavior were induced in the alignment direction, also yielding to high structural anisotropy. Conversely, mechanical performances in transversal direction to MF were weaker than those measured along the parallel direction to MF.

Furthermore, the use of a strong MF during the foaming process caused a complete reordering of microparticles along the MF direction. In this case, the mechanical properties were maximized in the MF directions but in the transversal direction to MF (because of the very low amount of reinforcing particles in the struts perpendicular to MF directions) they reduced to values comparable to those of the unreinforced foam.

The elastic modulus of the samples increased up to 340% in the MF direction (AH-Fe15 sample). At higher filler contents the reduction of mechanical properties, because of the increased expansion ratios prevailed on the reinforcing effect of the filler, although the mechanical properties of the matrix increased.

As suggested by the theoretical interpretations based on both Halpin-Tsai and Cox-Krenchel models for short fibers composites, the fibrillar structures,

even if formed by spherical particles, exhibited a reinforcement equivalent to that of solid short fibers.

The authors would like to thank Dr Lucia Mancini for providing 3D reconstruction from μCT images and Dr Vincenzo Scognamiglio for the contribution to all experimental activities.

References

1. Klempner, D.; Frisch, K. C. Polymeric Foams; Hanser: New York, 1991.
2. Throne, J. L.; Hinckley, O. H. Thermoplastic Foams; Sherwood Publishers: 1996.
3. Davis, J. M. Lightweight Sandwich Construction; Wiley-Blackwell: Oxford 2001.
4. Rusch, K. C. J Appl Polym Sci 1969, 13, 2297.
5. Rusch, K. C. J Appl Polym Sci 1970, 14, 1433.
6. Gong, L.; Kyriakides, S.; Jang, W. Y. Int J Solids Struct 2005, 42, 1355.
7. Gibson, L. J.; Ashby, M. F. Cellular Solids: Structure and Properties; 2nd ed.; Cambridge University Press: Cambridge, 1999.
8. Gong, L.; Kyriakides, S. Int J Solids Struct 2005, 42, 1381.
9. Pampolini, G.; Del Piero, G. J Mech Mater Struct 2008, 3, 969.
10. Shen, H.; Lavoie, A. J.; Nutt, S. R. Compos Part A Appl Sci Manuf 2003, 34, 941.
11. Yang, Z.-G.; Zhao, B.; Qin, S.-L.; Hu, Z.-F.; Jin, Z.-K.; Wang, J.-H. J Appl Polym Sci 2003, 92, 1493.
12. Alonso, M. V.; Auad, M. L.; Nutt, S. R. Compos Part A Appl Sci Manuf 2006, 37, 1952.
13. Goods, S. H.; Neuschwanger, C. L.; Whinnery, L. L.; Nix, W. D. J Appl Polym Sci 1999, 74, 2724.
14. Saint-Michel, F.; Chazeau, L.; Cavaille, J. Y. Compos Sci Technol 2006, 66, 2700.
15. Saint-Michel, F.; Chazeau, L.; Cavaille, J. Y.; Chabert, E. Compos Sci Technol 2006, 66, 2709.
16. Papathanaisou, T. D.; Ingber, M. S.; Guell, D. C. Compos Sci Technol 1995, 54, 1.
17. Vaidya, U. K.; Nelson, S.; Sinn, B.; Mathew, B. Compos Struct 2001, 52, 429.
18. Cartié, D. D.; Fleck, N. A. Compos Sci Technol 2003, 63, 2401.
19. Zangani, D.; Robinson, M.; Gibson, A. G.; Torre, L.; Holmberg, J. A. Plast Rubber Compos 2007, 36, 389.
20. Marasco, A. I.; Cartié, D. D.; Partridge, I. K.; Rezai, A. Compos Part A Appl Sci Manuf 2006, 37, 295.
21. Wang, B.; Wu, L.; Jin, X.; Du, S.; Sun, Y.; Ma, L. Mater Des 2010, 31, 158.
22. Potluri, P.; Kusak, E.; Reddy, T. Y. Compos Struct 2003, 59, 251.
23. Fan, X.; Xiao-Qing, W. Compos Struct 2010, 92, 412.
24. Kallio, M. The Elastic and Damping Properties of Magnetorheological Elastomers; VTT Publications: Espoo (Finland), 2005.
25. Jolly, M. R.; Carlson, J. D.; Munoz, B. C. Smart Mater Struct 1996, 5, 607.
26. Carlson, J. D.; Jolly, M. R. Mechatronics 2000, 10, 555.
27. Lanotte, L.; Ausanio, G.; Hison, C.; Iannotti, V.; Luponio, C.; Luponio, C. J Opt Adv Mater 2004, 6, 523.
28. Fuchs, A.; Rashid, A.; Liu, Y.; Kavlicoglu, B.; Sahin, H.; Gordaninejad, F. J Appl Polym Sci 2010, 115, 3348.
29. Engelmayr, G. C. Jr.; Mingyu Cheng; Bettinger, C. J.; Borenstein, J. T.; Langer, R.; Freed, L. E. Nat Mater 2008, 7, 1003.
30. Mathieu, L. M.; Mueller, T. L.; Bourban, P. E.; Pioletti, D. P.; Mullerb, R.; Manson, J. A. E. Biomaterials 2006, 27, 905.
31. Sorrentino, L.; Aurilia, M.; Iannace, S. Advance Science Technlogy, Vincenzini, P., D'Arrigo, G., Eds.; Trans Tech Publications: Switzerland, 2008; Vol. 54, p 123.
32. Halpin, J. C.; Kardos, J. L. Polym Eng Sci 1976, 16, 344.
33. Tucker, C. L.;Liang, E. Compos Sci Technol 1999, 59, 655.
34. Foster, R. J.; Hine, P. J.; Ward, I. M. Polymer 2009, 50, 4018.
35. Thomason, J. L.; Groenewoud, W. M. Compos A 1996, 21, 555.